Small Angle Neutron Scattering Study of the Magnetic Flux-Line Lattice in Single Crystal $2H$-$NbSe_2$

P. L. Gammel, D. A. Huse, R. N. Kleiman, B. Batlogg, C. S. Oglesby, E. Bucher,* and D. J. Bishop
AT&T Bell Laboratories, Murray Hill, New Jersey 07974

T. E. Mason† and K. Mortensen
Risø National Laboratory, 4000 Roskilde, Denmark
(Received 30 August 1993)

We report on a small angle neutron scattering study of the flux-line lattice in single crystal $2H$-$NbSe_2$. As the magnetic field is tilted away from the crystalline c axis, we find distortions in the flux lattice as would be expected for a mass anisotropy $\Gamma = 10.1 \pm 0.9$. However, we find that the lattice orientation is in disagreement with the predictions of both anisotropic London and Ginzburg-Landau theories. The observed flux lattice orientation remains pinned to that of the crystal lattice for the field orientations studied. The form factors can be quantitatively understood within the framework of Ginzburg-Landau corrections to the London equations.

PACS numbers: 74.60.Ec, 61.12.Ex, 74.60.Ge, 74.70.Ad

The magnetic flux-line lattice (FLL) in anisotropic superconductors has been found to possess many remarkable properties. Numerous novel static structures have been reported [1], especially for magnetic fields tilted away from the principal crystalline axes. Many of these observed structures disagree with the predictions of either uniaxial London or Ginzburg-Landau theories which *a priori* one would expect to be applicable. However, Bitter decoration and scanning tunneling microscopy (STM) studies only measure the FLL as it emerges from the surface of the crystal and have generally looked at rather thin, platelike samples. The interaction between flux lines is different at the surface than in the bulk [2], so there is the possibility that the flux patterns seen at the surfaces for such very thin samples may not accurately represent the flux patterns that would occur in the bulk of a large crystal.

In order to further explore this issue, we have used small angle neutron scattering (SANS) to study the behavior of the FLL in $2H$-$NbSe_2$. SANS has several advantages for this type of study. The first is that SANS probes the flux lines in the bulk of the material. The second is that the absolute reflectivity gives one substantial information about the flux-line structure through the measured form factors. For example, the reflectivity and rocking curve widths can determine whether flux lines bend or disorder as they traverse the thickness of the sample. Finally, the flux lines can easily be studied for applied fields at all orientations, including perpendicular to the c axis, a problematical direction for surface experiments. In contrast to YBCO, the only other superconductor with strong uniaxial anisotropy which has so far been studied [3] with SANS $2H$-$NbSe_2$ can now be grown into large single crystals without twins or other strong pinning centers. This system has a modest effective mass anisotropy $m_c/m_a = \Gamma = 10$ and has been widely studied in transport measurements [4]. For $B \parallel c$, the penetration depth is $\lambda(0) \sim 2000$ Å and the coherence length is $\xi(0) \sim 76$ Å. The flux lattice in this material has been studied with both STM [5] and Bitter decoration [6] over a large field range, making it an attractive choice for bulk studies of the magnetic FLL.

The large, very high quality single crystal [7] used in this experiment was faceted on all sides with dimensions of $4 \times 8 \times 1.1$ mm^3. X-ray studies confirmed the $2H$ polytype and determined the c axis mosaic to be less than 0.1° FWHM. Magnetization studies of this crystal showed a sharp $T_c(0) = 7.2$ K and $\partial H_{c2}/\partial T = 8.1$ kG/K for the field parallel to the c axis. The mass ratio for this crystal was determined to be $\Gamma = 9.5 \pm 1$ and the critical current measured to be < 1 A/cm^2. Transport studies on a slightly smaller sample grown at the same time showed a residual resistivity ratio (RRR) ~ 20 with $\rho_n(T_c) \sim 5$ $\mu\Omega$ cm. The transition width was found to be less than 20 mK at all fields. As in the magnetization studies, transport measurements found $T_c(0) = 7.2$ K and $\partial H_{c2}/\partial T = 7.9$ kG/K. For $B \parallel c$, the transport critical current was somewhat higher than that inferred from M-H loops, ranging up to 40 A/cm^2 at low fields. The critical current showed a very pronounced peak effect near $0.9H_{c2}$ as has been reported previously [8].

The SANS experiments were performed in the cold neutron guide hall of the Risø DR3 reactor. The sample was masked to expose a region $3 \times 6 \times 1.1$ mm^3 to the neutron beam. The incident neutrons had a wavelength of $\lambda_n = 10.0$ Å with a beam divergence of 0.1° FWHM matched to the neutron bandwidth $\Delta\lambda/\lambda = 0.18$. The diffracted neutrons were counted by an area detector at the end of a 6 m evacuated chamber. A horizontal magnetic field was applied along the beam direction using a superconducting magnet in the persistent mode. A specially designed low temperature rotation stage was used to allow us to rotate the sample with respect to applied magnetic field *in situ*, as shown in the inset of Fig. 2. The orientation of the crystal with respect to the applied field (8.0 kG for all the data reported here), was mea-

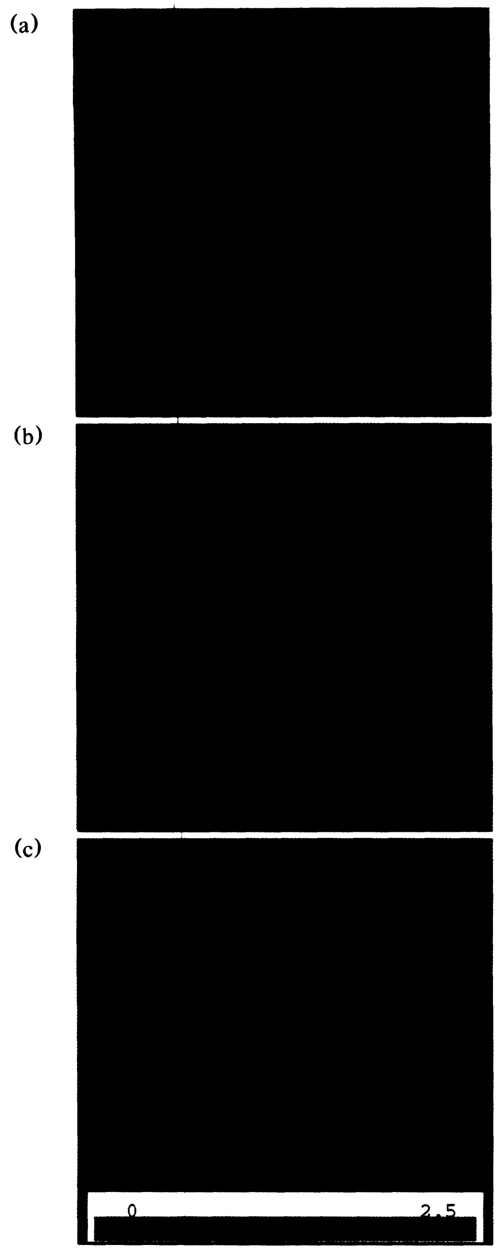

FIG. 1. The diffraction pattern of the FLL summed over the Bragg conditions for the six peaks with no background subtraction. The small angle scattering is due to stacking faults in the crystal. Both the distortions and changes in intensity are apparent as the field is rotated away from the c axis. The angles are (a) $\theta=0°$, (b) $\theta=56.8°$, and (c) $\theta=89.4°$. The intensity scale is normalized to the direct beam ($\times 10^5$) and is the same for all angles.

sured with a Hall probe attached to the stage. Independent identification of 0° and 90° was obtained from measurements of the transmission of the direct neutron beam through the sample mask and allowed absolute measurements of the angle of the applied magnetic field relative to the c axis to be made to within $\pm 0.1°$.

The primary experimental result is summarized in Fig. 1. Shown are diffraction patterns for three different rotation angles. Each pattern is the sum of scans at the Bragg condition for each of the six peaks at a temperature of 5.19 K. The data shown in Fig. 1 are the raw data with no background subtraction having been done. In Fig. 1(a), the field is applied parallel to the c axis; in Figs. 1(b) and 1(c) the angles between B and c are 56.8° and 89.4°, respectively. As can be clearly seen in the figure, the FLL distorts as the field is rotated away from the c axis. Despite this distortion, the orientation of the lattice remains fixed. As the lattice distorts, the reflections along the abcissa fall in intensity relative to the other four peaks. In this study, only the lowest order peaks were observed. In addition to the prominent flux lattice peaks, one can also see small angle scattering at low q presumably due to stacking faults in the crystal. This temperature independent background term shows a characteristic q^2 dependence as $q \rightarrow 0$ and the expected dependence with angle as the sample is rotated with respect to the incident neutron beam.

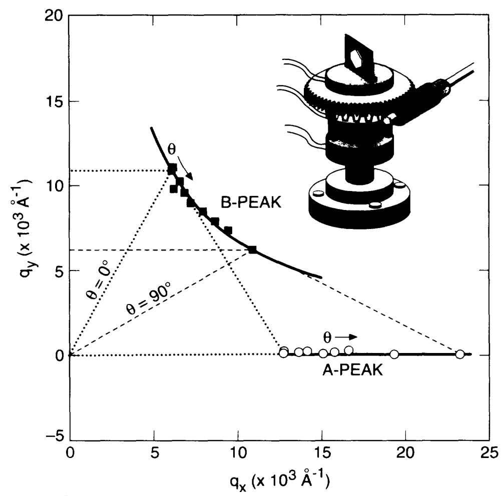

FIG. 2. The q values for the peaks are shown for all angles studied. The solid squares are an average over the four type B peaks and the open circles are an average over the two type A peaks. The London predictions for the trajectories are shown as the solid lines. In addition, one quadrant of the reciprocal lattice is shown for $\theta=0°$ (dotted lines) and $\theta=90°$ (dashed lines). The inset shows the rotation stage used for the experiment.

The diffraction patterns in Fig. 1 form a symmetric structure with two types of peaks. There are two peaks on the horizontal axis which move to larger q as a function of rotation of the magnetic field away from the c axis. These we call type A peaks. The other four peaks are also equivalent and these we call type B peaks. These peaks move closer to the horizontal axis as the field is rotated. Shown in Fig. 2 is the averaged scattering wave vector for these two types of peaks as a function of rotation angle. For $B \parallel c$, the diffraction peaks from the FLL form a perfect hexagon (sketched with dotted lines in Fig. 2) with scattering wave vector $q_0=0.0128$ Å^{-1}, which is

$\sim \frac{1}{2}$ detector pixel lower than the estimated value of $q = 2\pi(2B/\sqrt{3}\phi_0)^{1/2} = 0.0132$. This is within our measurement error. For $B \parallel c$, all six peaks have equal rocking curve widths of 0.17° (FWHM), which are resolution limited and consistent with the measured bound on the crystalline c axis mosaic. The orientation of the diffraction shows that the FLL is aligned with the crystalline a axis.

The averaged peak intensity for $B \parallel c$ shows a temperature dependence $I \sim [T - T_c(H)]^2$ which agrees with the temperature dependence in mean-field (Ginzburg-Landau) theory. A fit of the temperature dependent intensity to find $T_c(H = 8.0 \text{ kG})$ implies $\partial H_{c2}/\partial T = 7.6 \pm 0.5$ kG/K in agreement with both transport and magnetization studies.

For magnetic fields applied at an angle to the c axis, the lattice distorts but maintains its orientation with respect to the underlying crystalline structure. In general, the FLL Bragg peaks lie on an ellipse, and we define the distortion as the ratio of the minor to the major axis of this ellipse. Data taken as a function of tilt angle were fitted to ellipses and the distortions are plotted in Fig. 3 as a function of angle. Within the framework of London theory [9], one expects that the distortion should follow the functional form $(\text{distortion})^2 = (1 - 1/\Gamma)\cos^2\theta + 1/\Gamma$. As shown in the figure, the data follow this functional form quite well with $\Gamma = 10.1 \pm 0.9$. London theory also predicts the trajectories in q space for the Bragg peaks as a function of rotation angle. Shown in Fig. 2 as the solid lines are the predicted trajectories for the A and B peaks as a function of angle. For the A peak, the trajectory should be $q_x/q_0 = \varepsilon^{-1/4}$ and $q_y/q_0 = 0$, where $\varepsilon(\theta) = \Gamma^{-1} \times \sin^2(\theta) + \cos^2(\theta)$. For the B peak, the trajectory is expected to be $q_x/q_0 = (\varepsilon^{-1/4})/2$ and $q_y/q_0 = \varepsilon^{1/4}\sqrt{3}/2$. The data are seen to be in good agreement with these predicted trajectories. Angle dependent studies with STM yielded an appreciably smaller value $\Gamma \sim 7$, well outside our error. This disagreement may be a sign of FLL distortion at the surface of the crystal.

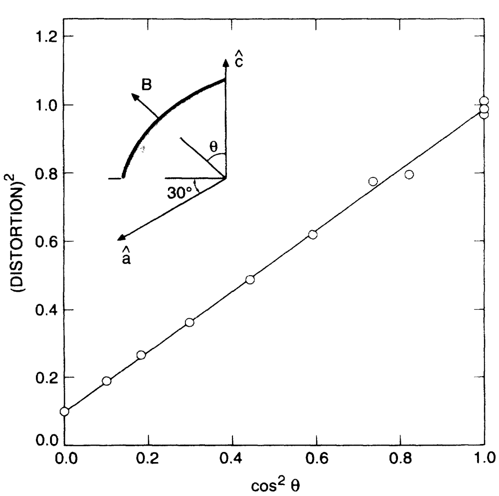

FIG. 3. The distortion of the hexagonal lattice is shown. The $\cos^2\theta$ dependence follows from the London equations. The slope and intercept give $m_c/m_a = 10.1 \pm 0.9$. In the inset, the tilt used in this experiment is shown.

Shown as an inset to Fig. 3 is a sketch of the orientation of the field with respect to the crystal. With an in-plane projection of the field 30° away from the a axis, both London [9] and Ginzburg-Landau [10] calculations would predict that the FLL should rotate away from the a axis to align with the in-plane projection of the magnetic field. However, the energy driving this effect is small [11], with a free energy difference δF between the two orientations given by $\delta F/F = 10^{-3}(\phi_0/B\lambda^2)f(\theta)$. In this expression, $f(\theta)$ is an expression of order unity, vanishing at $\theta = 0°$ and $\theta = 90°$.

The data presented here show, as has been seen in surface experiments [5,6] on $2H$-$NbSe_2$, that the FLL remains locked to the crystal lattice for all orientations. Therefore the intrinsic pinning in this material must be at least as strong as the London free energy terms estimated above. Similarly oriented lattices have also been seen [12,13] in UPt_3 and technetium, but only for $\theta = 90°$, where the two lattice orientations are degenerate in energy within the London approximation. Interestingly, for large angles the corrections due to surface terms favor the observed lattice orientation [6,14]. In YBCO, however, the lattice predicted by the London equations is seen in both decoration [15] and neutron scattering [3]. The reason for this difference is unclear but it may be related to the large range of vortex liquid in YBCO.

The observed orientation of the FLL in this system still leaves some open questions. Consider the shaded triangle on the sphere of orientations of B as shown in the inset of Fig. 3. We have measured the orientation and distortion of the flux lattice along the edge with the solid line and find a continuous, smooth rotation of the lattice there. However, if we postulate a similar smooth rotation along the other two edges of the triangle, the resulting orientation when the field is parallel to a is different depending on whether one (i) rotates 90° from c straight to a or (ii) rotates 30° about c from the other corner of the triangle. Thus there must be a phase transition in the equilibrium orientation of the flux lattice along one of the edges of this triangle. The STM [16] studies suggest that this phase transition occurs along the edge between c and a. A related orientational transition has been observed [17] in pure Nb.

Finally, one can obtain significant information from the reflectivities of the FLL diffraction peaks. Shown in Fig. 4 are the averaged peak intensities for the type A and B peaks as a function of tilt angle. For $B \parallel c$, the reflectivity can be expressed [18] as $R = (2\pi\gamma^2\lambda_n^2 t/16\phi_0^2 q)H_1^2$, where $\gamma = 1.91$ is the neutron gyromagnetic ratio and t is the sample thickness. The form factor H_1 has the units of a magnetic field. Since these experiments are performed at $H/H_{c2} \sim 0.5$, there is a substantial G-L correction to the form factor. Using only the leading order correction [19]

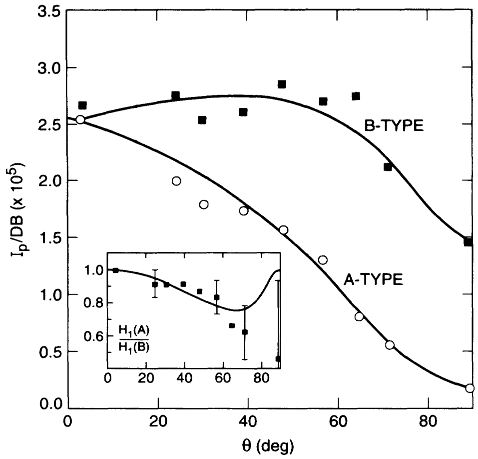

FIG. 4. Shown are the intensities of the A type peaks (open circles) and B type peaks (closed squares) normalized to the direct beam as a function of angle. The lines are guides to the eye. In the inset, the ratio of the form factors for the two types of peaks are shown. The form factors are in qualitative agreement with the London expression shown as the solid line.

gives $H_1=(\phi_0/\lambda^2)(\sqrt{3}/8\pi^2)\exp(-4\pi^2B\xi^2/\sqrt{3}\phi_0)$. Using the extrapolated values of $\lambda(T)=0.52$ μm and $\xi(T)=0.02$ μm gives $H_1^2=3.2\times10^{-3}$ G^2 consistent with the value of $H_1^2=4.3\pm2\times10^{-3}$ G^2 extracted from the data.

As the field is rotated away from the c axis the relative intensities of the type A and B peaks change. Shown in the inset of Fig. 4 is the ratio of the form factors for the type A and B peaks. The solid line is the London limit [20] expression

$$[H_1(A)/H_1(B)]^2=1+[3(1-1/\Gamma)^2\sin^2\theta \times\cos^2\theta/\varepsilon(1+3\varepsilon)] .$$

In general, this expression provides a good fit over most of the range, but shows substantial deviations from the data at the highest angles. There are several factors which could contribute to this deviation from the London prediction. In the analysis of our data, we have assumed equal rocking curve widths for the A and B peaks to calculate the integrated intensities leading to the reflectivities. At high tilt angles, the type A peaks are difficult to resolve, leading to a factor of 2 uncertainty in their widths. To reconcile the data with the London expression would require that the type A widths would have to be enhanced by a factor of 4 relative to the type B width at $\theta=90°$. However, one would naively expect, based on the anisotropic shear modulus [21], that the type A peaks would be narrower than the type B. The exact form factors at high angles still need to be understood.

In conclusion, we have presented data taken using SANS to study the FLL in $2H$-$NbSe_2$. As the magnetic field is rotated away from the c axis, the lattice distorts, as predicted within the effective mass approximation. However, the orientation of the lattice remains pinned to the crystallographic a axis. Such an orientation runs counter to both London theory and Ginzburg-Landau theory estimates for the minimum free energy. The form factors for the diffraction peaks can be modeled in detail using G-L corrections to the London equations.

We would like to thank E. D. Isaacs for x-ray data on this crystal, H. Safar for transport data, and V. G. Kogan for numerous helpful discussions. We also acknowledge the generous assistance of the Risø technical staff. This program was aided by grants from the Danish Natural Science Foundation.

*Also at Fakultat fur Physik, University of Konstanz, Konstanz, Germany.
†Present address: Department of Physics, University of Toronto, Toronto, Canada M5S 1A7.

[1] For a review, see D. J. Bishop *et al.*, Science **255**, 165 (1992).
[2] D. A. Huse, Phys. Rev. B **46**, 8621 (1992); M. C. Marchetti and D. R. Nelson (to be published).
[3] M. Yethiraj *et al.*, Phys. Rev. Lett. **70**, 857 (1993); E. M. Forgan *et al.*, Physica (Amsterdam) **185–189C**, 247 (1991); Nature (London) **343**, 735 (1990).
[4] For a recent study, see S. Battacharya and M. J. Higgins, Phys. Rev. Lett. **70**, 2617 (1993), and references therein.
[5] H. F. Hess, C. A. Murray, and J. V. Waszczak, Phys. Rev. Lett. **69**, 2138 (1992).
[6] C. A. Bolle *et al.* (to be published).
[7] C. S. Oglesby *et al.*, J. Cryst. Growth (to be published).
[8] P. Koorevaar *et al.*, Phys. Rev. B **42**, 1004 (1990); T. W. Jing and N. P. Ong, Phys. Rev. B **42**, 10781 (1990).
[9] L. Campbell *et al.*, Phys. Rev. B **38**, 2439 (1988); L. L. Daemon, L. J. Campbell, and V. G. Kogan, Phys. Rev. B **46**, 3631 (1992).
[10] K. G. Petzinger and G. A. Warren, Phys. Rev. B **42**, 2023 (1990).
[11] V. G. Kogan (private communication).
[12] R. N. Kleiman *et al.*, Phys. Rev. Lett. **69**, 3120 (1992).
[13] J. Schelten *et al.*, J. Low Temp. Phys. **14**, 213 (1974).
[14] V. G. Kogan, A. Yu. Simonov, and M. Ledvij, Phys. Rev. B **48**, 392 (1993).
[15] P. L. Gammel *et al.*, Phys. Rev. Lett. **68**, 3343 (1992).
[16] H. F. Hess (unpublished).
[17] D. K. Christen *et al.*, Phys. Rev. B **21**, 102 (1980).
[18] J. Schelten *et al.*, Phys. Status Solidi B **48**, 619 (1971); M. P. Kemorlidze, Zh. Eksp. Teor. Fiz. **47**, 2247 (1964) [Sov. Phys. JETP **20**, 1505 (1965)].
[19] E. H. Brandt, Phys. Status Solidi B **51**, 345 (1972).
[20] V. G. Kogan, Phys. Lett. **85A**, 298 (1981).
[21] G. J. Dolan *et al.*, Phys. Rev. Lett. **62**, 2184 (1989); V. G. Kogan and L. J. Campbell, Phys. Rev. Lett. **62**, 1552 (1989).

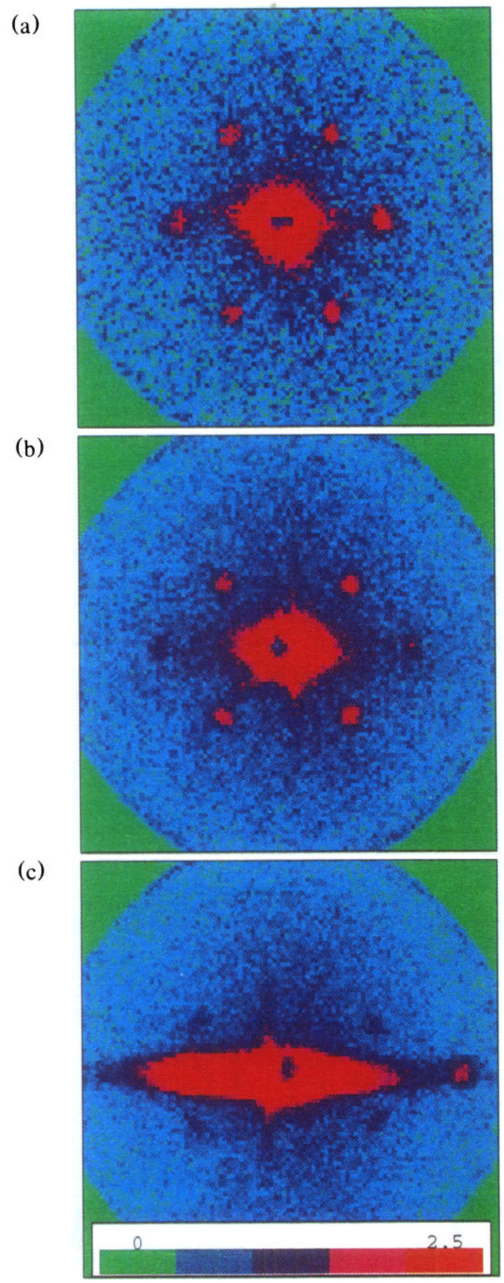

FIG. 1. The diffraction pattern of the FLL summed over the Bragg conditions for the six peaks with no background subtraction. The small angle scattering is due to stacking faults in the crystal. Both the distortions and changes in intensity are apparent as the field is rotated away from the c axis. The angles are (a) $\theta=0°$, (b) $\theta=56.8°$, and (c) $\theta=89.4°$. The intensity scale is normalized to the direct beam ($\times 10^5$) and is the same for all angles.

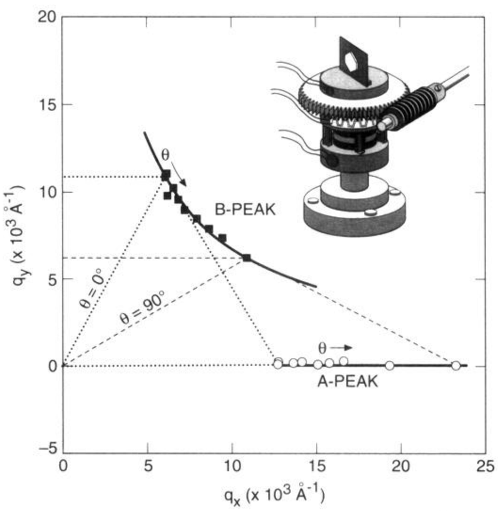

FIG. 2. The q values for the peaks are shown for all angles studied. The solid squares are an average over the four type B peaks and the open circles are an average over the two type A peaks. The London predictions for the trajectories are shown as the solid lines. In addition, one quadrant of the reciprocal lattice is shown for $\theta=0°$ (dotted lines) and $\theta=90°$ (dashed lines). The inset shows the rotation stage used for the experiment.

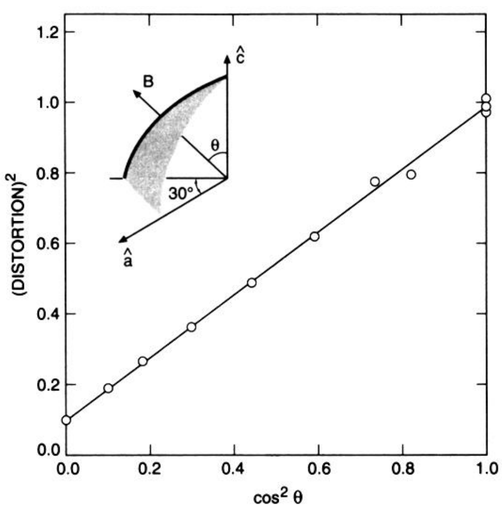

FIG. 3. The distortion of the hexagonal lattice is shown. The $\cos^2\theta$ dependence follows from the London equations. The slope and intercept give $m_c/m_a = 10.1 \pm 0.9$. In the inset, the tilt used in this experiment is shown.